Influence of Shielding Gas Composition on Weld Structure in Pulsed Nd: YAG Laser Welding

M. Jokar[a], F.Malek Ghaini[*a], M. J. Torkamany[a, b]
[a] *Department of Engineering Materials, Tarbiat Modares University, Tehran, Iran*
[b] *Iranian National Centre for Laser Science and Technology (INLC), PO Box: 14665-576, Tehran, Iran*

ARTICLE INFO

Article history:

Received 2 Sep 2012
Accepted 12 Jan 2013
Available online 20 November 2013

Keywords:

Laser welding
Pulsed Nd: YAG laser
Argon shielding gas
Carbon dioxide
Weld microstructure

ABSTRACT

This work studied the effect of additions of carbon dioxide to argon shielding gas on the weld shape and microstructure of ST14 steel in pulsed Nd: YAG laser welding. By additions of carbon dioxide up to 15%,the weld area and depth/width ratio decreases while rising of carbon dioxide up to 25% causes increasing of weld area and depth/width ratio. It is observed that the weld metal microstructure is mainly constructed from polygonal ferrite under 0 to 15% CO_2 additions to argon, but both polygonal and acicular ferrites are observed as the CO_2 level of Ar+ CO2 mixtures increases from 15 to 25%. The shape and microstructure of pulsed Nd: YAG laser welds is believed to be closely related to laser absorption coefficient, laser energy absorption on the work-piece surface and formation of oxide layer on the work-piece surface.

1. Introduction

Laser welding is widely popular in modern technology and industry due to the high speed of the process, easy controllability, high input thermal density, and small heat affected zone [1]. Nowadays laser welding systems are used in many automobile manufacturing companies [2]. Automation and high speed are the main factors for using laser welding in automobile industries [2]. Because of its short wavelength (1.06 μm) and less reflectivity from the surface of metals, pulsed laser welding can be more useful than CO_2 laser welding with 10.6 μm wavelength [3]. On the other hand, pulsed laser welding as an economic and new technology can be effectively used for a fast, clean and high-quality welding of auto body [4]. In laser welding, physical and metallurgical properties can be controlled by laser parameters such as pulse energy, maximum strength, focal point location as well as shielding gas parameters such as gas flow rate, composition of shielding gas and geometrical characteristics of shielding gas nozzle [3].

During laser welding, the interaction of laser beam and base metal results in heating and rapid melting of base metal. The temperature of molten metal in the center of interaction area reaches to temperatures higher than boiling point of base metal.

Corresponding author:
E-mail address: f.malekghaeini@gmail.com (Farshid Malekghaeini).

Therefore, the equilibrium pressure on the surface of molten pool is much higher than atmosphere pressure and as a result the elements in base metal evaporate with a relatively high rate [5]. Gas atoms in laser beam path areexcited or ionized and weld plasma is formed. Weld plasma consists of neutral, excited and ionized atoms of base metal and shielding gas [6]. Plasma plume absorbs some portion of laser beam energy and causes refraction and defocusing of laser beam [6]. In laser welding, shielding gas is generally used for protection of molten pool against atmosphere and hence prevention of oxidation of weld metal, as well as protection of laser lenses against spattering of molten metal and the plasma formed above the molten pool [7]. During welding because of the high temperature of molten pool surface and high pressure of weld atmosphere (weld plasma), there is a high possibility of solution and reaction of components present in plasma with molten metal [6]. The amount of laser beam absorption on the surface of base metal is dependent on surface conditions, temperature and density of laser beam energy [3]. Formation of an oxide layer on the surface dramatically decreases the amount of laser beam absorption [8, 9]. Therefore, shielding gas can influence laser beam absorption by weld metal surface through affecting plasma and the molten pool surface. Also, metallurgical and mechanical properties of weld metal are relatively influenced by the reaction between molten pool and the shielding gas.

The use of shielding gas with appropriate composition can influence the resulted weld characteristics by affecting plasma properties and interaction with weld metal [10, 11]. Gases with higher ionization potential energy cause decrease of electron density, decrease of plasma absorption coefficient and better focusing of laser beam [12]. In copper and copper-nickel alloy welding, addition of oxygen to the composition of shielding gas results in formation of an oxide layer on the metal surface and hence causes better laser beam absorption and increase of penetration depth [5, 9]. The effect of addition of CO2 on weld properties in gas metal arc welding (GMAW) method has been investigated and it has been revealed that with increase of CO2 percentage, penetration depth and weld toughness increase [11].

In stainless steel welding by gas tungsten arc (GTA) method it has been observed that by addition of CO2 and oxygen to argon shielding gas, at first the weld depth/width ratio increases due to solution of oxygen in weld metal and the change of Marangoni convection to inward direction, but with increase of these gases the weld depth/width ratio decreases because a thick oxide layer is formed on the surface of weld metal and Marangoni convection would change to the outward direction [13, 14]. Also, some researchers have studied the use of nitrogen and carbon dioxide in continuous laser CO2 welding and it has been observed that the use of carbon dioxide causes deterioration of mechanical properties due to formation of porosities in the weld, but composition of 50% argon plus 50% nitrogen results in favorable mechanical properties [10, 15]. The use of carbon dioxide in shielding gas composition is economically justified because of its relatively low cost. In pulsed Nd: YAG laser welding, the duration of stability of weld metal at high temperatures is low because of very high heating and cooling rate [16]. Therefore, it can be predicted that interaction between molten pool and shielding gas is very low, therefore active gases can be used in the composition of shielding gas. In this research, the effect of different percentages of CO2 in argon shielding gas composition on morphology and microstructure of pulsed Nd: YAG laser weld has been investigated.

2. Materials and research methodology

Low carbon ST14 steel plate (10×5cm, 2mm thick) with chemical composition corresponding to table 1 was used as welding work-piece.

Table1. Chemical composition of the steel plate (weight percent)

Element (%)	C	Mn	P	S	Fe
Percent	0.04	0.22	0.006	0.006	Base

An IQL-10 Nd: YAG pulsed laser with a maximum mean laser power of 400W was used. This laser can produce square shape pulses with 0.2-20ms pulse width and 1-1000Hz frequency with maximum 40J energy. Any composition of these parameters can be used provided that the output power of laser does not exceed 400W. Also, a focalizing setup with 75mm focal lengthwas used forfocusing the laser beam. Minimum diameter of laser spot attainable in this laser instrument is 25µm. An OPHIR LP-5000W power meter and LP-LA300W joule meter were used for measuring power and energy of the laser pulse. Also, in order to prevent the possible movement of the samples a special clamp for holding the samples during welding process was used. A table which could move along X, Y and Z orientations with 0.05mm precision for moving of the work-piece at the specified speed under the immobile narrow laser focal point was also used. Argon (99/9% purity) and carbon dioxide (99% purity) were used in composition of the shielding gas. The shielding gas was blown on welding zone by a nozzle which was coaxial with laser beam. To measure the gas flow rate, Officine Orobicherotameters were used and for mixing the gases a 3-way mixing valve was used. Laser parameters and shielding gas composition used in 6 test series are shown in tables 2 and 3, respectively. 5cm-long welding was carried out by sheet welding method. Prior to welding process the samples were cleaned by abrasive paper and then washed by acetone. To study dimensional variations of weld metal, three metallographic samples from the surface of weld cross section were chosen and cut along the weld midline. The chosen samples were studied and analyzed by Olympus DP25 optical microscope after polishing and carving in 3% nitalsolution. Image Tool software was used for precise measurement of weld dimensions and area. Average ferrite grain size was measured according to ASTM E112 standard.

Table2. Welding condition

Pulse duration (ms)	Frequency (Hz)	Welding speed (mm/s)	average power (W)	Shielding gas flow rate (Lit/min)
7	20	4	220	60

Table3. Shielding gas composition

sample codes	shielding gas composition
A	Ar
B	95%Ar+5%CO2
C	90%Ar+10%CO2
D	85%Ar+15%CO2
E	80%Ar+20%CO2
F	75%Ar+25%CO2

3. Results and discussion

3.1. Dimensional studies of the weld

Weld cross sections of samples A (100%Ar), D (85%Ar+15%CO2) and F (75%Ar+25% CO2) are sequentially presented in figs 1a-c. Fig 2 shows the weld area versus CO2 concentration in shielding gas. As can be seen in fig 2, with increase of CO2 up to 15%, the molten pool area (indicator of energy absorbed by work-piece) decreases to 39% (region 1); whereas with increase of 15 to 25% of CO2,weld area increases up to 72% (region 2). The reason can be found in the effect of carbon dioxide on absorption coefficient, oxidation of molten pool surface and Marangoni convection of molten metal.

During laser welding the energy passed from plasma is calculated by the following equation:

$$I(h) = I_0(1-R)e^{-\alpha h} \qquad (1)$$

Where I(h) is laser beam intensity at the moment of reaching the work-piece, I0 is the primary intensity of laser beam, R is coefficient of laser beam reflection from base

metal surface, α is the inverse Bremsstrahlung absorption coefficient, and h is the height of laser beam and plasma fusion zone. Energy needed for decomposition of CO2 molecule is 5.5 eV, which is lower than ionization potential energy of argon 15.15 eV [18].

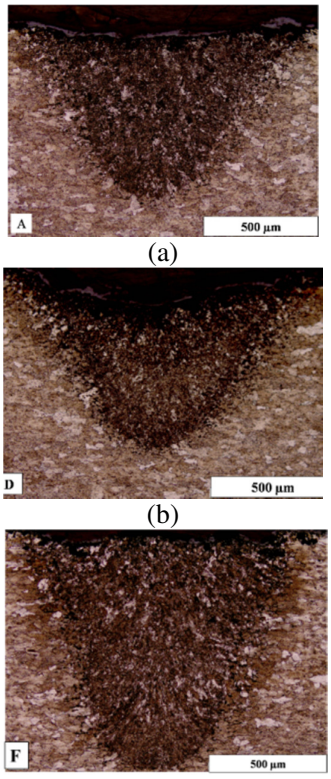

Fig.1. Welds produced with different mixtures of argon and carbon dioxide as shielding gas: a) A (100% Ar), b) D (85% Ar + 15% CO2), c) F (75% Ar + 25% CO2)

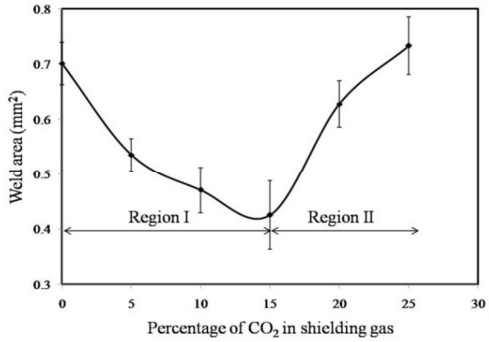

Fig.2. Weld area versus CO2concentration in shielding gas

With increase of CO2 concentration in the shielding gas the inverse Bremsstrahlung coefficient increases [12]. As a result, according to equation (1), lower energy reaches the work-piece surface; therefore, decrease of weld area is expected. Thus, the decrease of weld area in region 1 can be related to the dominating effect of plasma absorption coefficient.

On the other hand, oxygen and carbon resulted from CO2 decomposition in plasma atmosphere can react with weld metal and change the weld properties. Due to high temperature of laser welding plasma, CO2 can be decomposed according to the following reactions:

$$CO_2 + 25eV = C^+ + O_2 \quad (2)$$

$$CO_2 + 28.4eV = C^+ + 2O \quad (3)$$

$$CO_2 + 19eV = O^+ + CO \quad (4)$$

The researches carried out on nitrogen solubility reveal that nitrogen solubility in molten metal in the presence of plasma is more than normal state [19]. This phenomenon can be explained by the fact that in plasma atmosphere, electrons are heated to much higher temperatures due to their much lower inertia compared to ions. Therefore, mobility of electrons is higher than other components and as a result the flux of electrons toward the molten surface is much greater. As it is shown schematically in fig 3, the electrons hit the molten surface with a high speed and cause the formation of negative charge on the surface and plasma with positive charge is located above it. The presence of attraction between positive ions and the surface with negative charge causes the increase of ions solubility in molten phase [20].

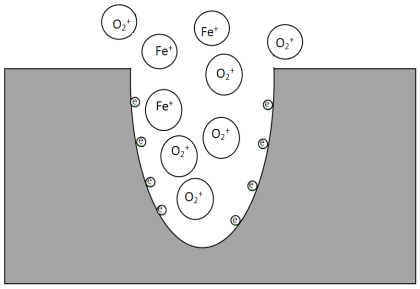

Fig.3. Schematic representation of the plasma-weld pool interaction

According to equations (2-4) the possibility of oxygen ions formation is higher than carbon. On the other hand, because of the negative charge on molten pool surface the possibility of ion… is more than the neutral ones. Also, reactivity of oxygen with iron is higher than carbon with iron [18]. Therefore, the reaction of carbon with weld metal and its effect on composition and structure of weld metal can be neglected. Oxygen ion attracts the surface electron after contact with the surface and becomes stable. The reaction of oxygen with iron results in formation of iron oxide according to equation (5). For this reaction in any temperature, Gibbs free energy must be smaller than zero (equation 6) [21].

$$Fe + O = FeO \quad (5)$$

$$\Delta G = \Delta G^0 - R\,T\,Ln P_{O_2}^{1/2} < 0 \quad (6)$$

Where ΔG, ΔG0, R and T are Gibbs free energy, standard Gibbs free energy, gas constant and absolute temperature, respectively. Therefore, in any temperature the necessary condition for iron oxide formation is the establishment of equation (7).

$$P_{O_2} > \frac{\Delta G^0}{RT} \quad (7)$$

In other words, for oxidation the partial pressure of oxygen must be higher than a certain limit. Fig4a-c shows the images of surface appearance of samples A (100%Ar), D (85%Ar+15%CO2) and F (75%Ar+25%CO2) after brushing and cleaning by acetone. As can be seen, with increase of CO2 up to 15%, weld surface appearance has not changed too much (fig 4a-b), but after that the weld surface has been intensively darkened and spattering has increased (fig 4c). It can be concluded that for the amounts more than 15% CO2, partial pressure of oxygen resulted from decomposition of CO2 is more than critical amount and oxidation occurs which releases some energy. Moreover, the oxide produced on the surface causes the increase of laser absorption on base metal surface [9]. Therefore, the increase of weld area in the second region of fig 2 can be related to the appearance of oxide layer in this region.

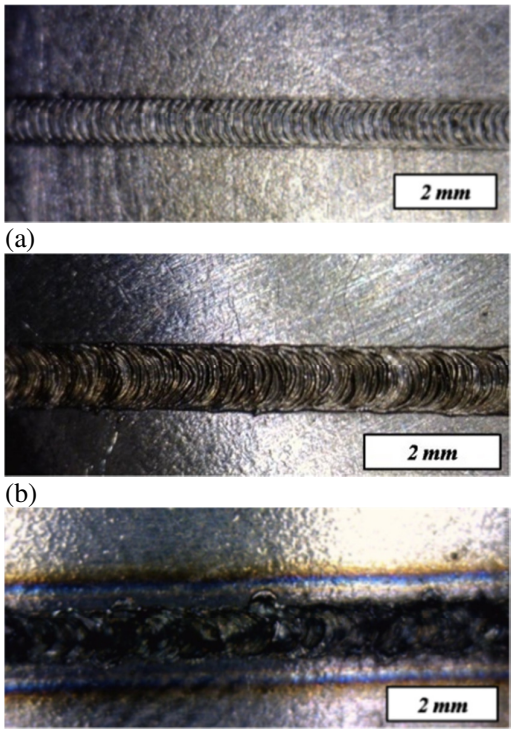

(a)

(b)

(c)

Fig.4. weld surface appearance of: a) A (100% Ar), b) D (85% Ar+15% CO2), and c) F (75% Ar+25% CO2

Variations of depth/width ratio can be another sign of oxidation in the second region of fig 2. For many materials, in the absence of active elements in the surface, the ratio of surface tension to temperature variations is negative. In other words, with increase of temperature the surface tension decreases. Therefore in the molten pool surface the melt flows toward the borders, because the warmer melt has lower

tension stress and is pulled by the border melt with higher tension stress. As a result of this phenomenon, the melt moves toward the borders and the weld takes a relatively shallow, wide shape [13, 14]. If surface active elements such as oxygen and sulfur be present in the molten pool surface, the ratio of surface tension to temperature variations becomes positive, therefore the melt moves from the borders toward the weld center and the resulted weld is relatively deep and narrow.

Fig 5 shows depth/width ratio of weld versus CO2 concentration. Generally, with increase of a gas with lower ionization potential, the focus of laser beam decreases and the decrease of depth/width ratio is expected [6]. In region 1 ($0 \leq CO2 \leq 15$) the depth/width ratio has 16% decrease which can be due to the increase of electron density and deviation of laser beam. But in region 2 ($15 < CO2 \leq 25$) the depth/width ratio has 56% increase. Therefore it can be claimed that in region 2 ($15 < CO2 \leq 25$) the presence of oxygen in the molten pool surface has caused the increase of area as well as the weld depth/width ratio.

3.2. Microstructural studies of the weld

Fig 6a-d shows the weld structure in four samples A (100%Ar), D (85%Ar+15%CO2), E (80%Ar+20%CO2) and F (75%Ar+25%CO2) in 1000x magnification. In fig 6a&b it is observed that the weld structure of samples A (100%Ar) and D (85%Ar+15%CO2) is made up of the predominating phase of polygonal ferrite with mean linear size 7±0.5µm and 6±0.5µm, respectively. This difference of grain size can be related to the higher cooling rate of sample D which decreases the grain growth. But in fig 6c&d it can be seen that weld structure of samples E (80%Ar+20%CO2) and F (75%Ar+25%CO2) is composed of polygonal and acicular ferrite. Oxide precipitations are usually appropriate locations for nucleation of acicular ferrite. It can be said that in samples E and F oxide precipitations caused the formation of acicular ferrite in weld structure.

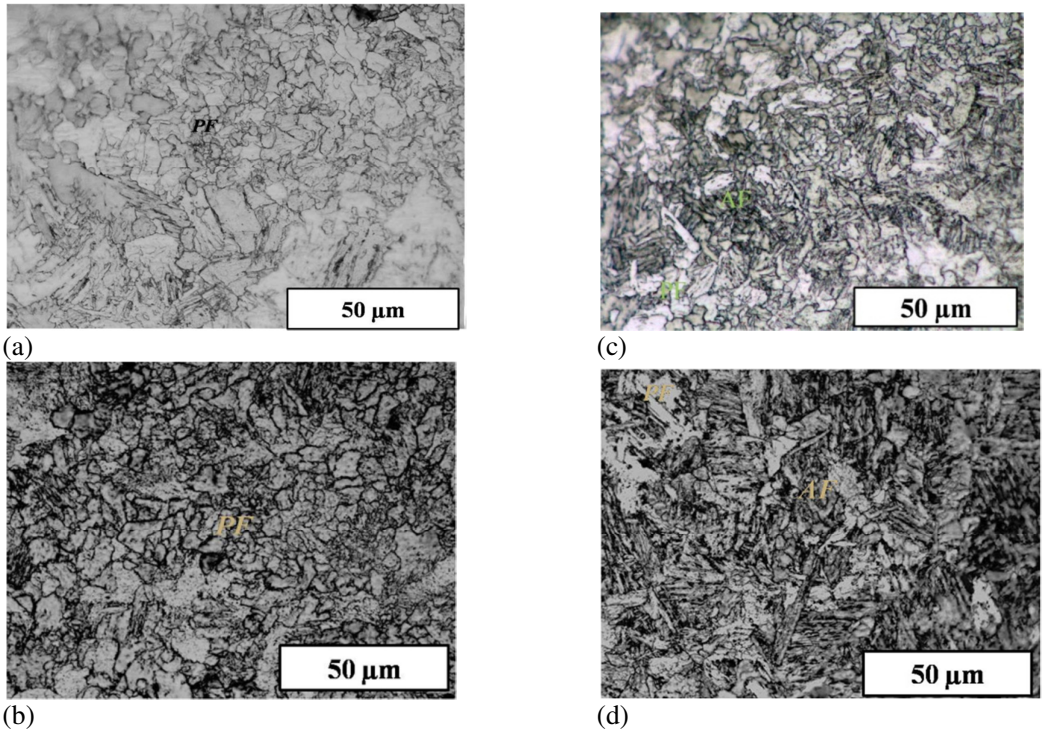

Fig.6. Weld pool microstructures of: a) A (100% Ar), b) D (85% Ar+15% CO2), c) F (80% Ar+20% CO2) and d) F (75% Ar+25% CO2), AF: acicular ferrite, PF: polygonal ferrite.

In these experiments it was observed that in low carbon steel Nd: YAG pulsed laser welding, the HAZ structure is relatively more refined than base metal structure and coarsening grain region is not formed in heat affected zone. Fig 7 shows base metal structure (mean linear size 38±0.5μm) and heat affected zone (mean linear size 17±0.5μm) and weld metal taken from sample A (100%Ar). By using the Fe-C phase diagram in low-carbon steels the HAZ can be divided into three regions: partial grain-refining, grain-refining and grain-coarsening regions. This division depends on the temperature peak of that region and duration of stability in high temperatures [22].

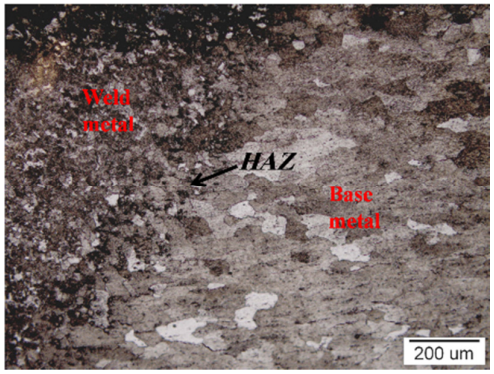

Fig.7. Weld structure of a sample (100%Ar)

A portion of the base metal which changes into heat affected zone undergoes two transformations: ferrite-to-austenite and austenite-to-ferrite. These transformations require nucleation and development of the new phase in the initial phase [23]. The structure of such transformations depends on temperature peak, primary structure and heating and cooling rates. With increase of temperature peak, the primary grain size and heating rate, austenite structure (in high temperature) as well as the final structure is expected to be coarse. On the other hand, cooling rate usually has a reverse effect [24]. Since nucleation process precedes growth, and since in growth process the absorption occurs in a larger domain, dependence of growth on duration is higher. Cooling rate in Nd: YAG pulsed laser welding is much higher than conventional welding methods [16], therefore the absence of formation of coarsening-grain region in heat affected zone in Nd: YAG pulsed laser welding could be related to the rapid heating and cooling rates of this laser, in which there is no sufficient time for growth of austenite grains and formation f coarsening-grain region in HAZ.

4. Conclusion

Based on the studies, the properties of pulsed laser Nd: YAG weld change by variations in shielding gas composition. By addition of CO2 to argon shielding gas the weld can be divided into two regions. In region 1($0\leq CO2\leq 15$) weld structure is mainly composed of polygonal ferrite and with increase of CO2 concentration the grain size, area and depth/width ratio of the weld show a decrease of 39% and 16%, respectively. In region 2 ($15<CO2\leq 25$) weld structure is made up of polygonal and acicular ferrite and with increase of CO2 in shielding gas composition the weld area and depth/width ratio show an increase of 72% and 56%, respectively. Also, in pulsed Nd: YAG laser welding the coarsening-grain region is not formed in HAZ structure.

5. Acknowledgment

The authors are thankful for the assistance of the Iranian National Centre for Laser Science and Technology, especially Mr. Ali Chehreghani.

6. References

[1] M.Yasunobu, H. Koji, K. Yukihisa, K. Junichi, “Welding Methods and Forming Characteristics of Tailored Blanks (TBs)”. Nippon Steel Technical Report, No. 88, 2003, pp. 39–43.

[2] D. Ashish, V. Jyoti, “A Novel Method for Lap Welding of Automotive Sheet Steel Using High Power CW CO2 Laser”. Proceedings of the 4th International Congress on Laser Advanced Materials Processing.

[3] K.A. Elijah, Principles of laser materials processing. John Wiley & Sons, New Jersey, 2009.

[4] F. MalekGhaini, M.J. Hamedi, M.J. Torkamany, J. Sabbaghzadeh “Weld metal microstructural characteristics in pulsed Nd:

YAG laser welding". ScriptaMateriali 56, 2007, pp. 955-958.
[5] M.C. Collur, "Alloying element vaporization and emission spectroscopy of plasma during laser welding of stainless steels". PhD Thesis, Pensilvania State University, 2008.
[6] M. Beck, P. Berger, H. Hugel "The effect of plasma formation on beam focusing in deep penetration welding with CO2 lasers". J. Phys. D: Appl. Phys, 28, 1995, pp. 2430-2449.
[7] D. Grevey, P. Sallamand, E. Cicala, S. Ignat "Gas protection optimization during Nd:YAG laser welding", Optics & Laser Technology, 37, 2005, pp. 647-651.
[8] S. Dadras, M.J. Torkamany, J. Sabbaghzadeh, "Spectroscopic characterization of low-nickel copper welding with pulsed Nd:YAG laser". Optics and Lasers in Engineering, 46, 2008, pp. 769–776..
[9] E. Biro, D.C. Weckman, Y. Zhou, "Pulsed Nd:YAG Laser Welding of Copper Using Oxygenated Assist Gases". Metall Mater Trans A, 2002, 33, 2002, pp.2019–2030.
[10] B.G. Chung, S. Rhee, C.H. Lee, "The effect of shielding gas types on CO2 laser tailored blank weldability of low carbon automotive galvanized steel", Materials Science and Engineering, A272, 1999, pp. 357–362.
[11] M. Ebrahimnia, M. Goodarzi, M. Nouri, M. Sheikhi, "Study of the effect of shielding gas composition on the mechanical weld properties of steel ST 37-2 in gas metal arc welding". Materials and Design, Vol.30, 2009, pp.3891–3895.
[12]M. Glowacki, "The effects of the use of different shielding gas mixtures in laser welding of metals". J. Phys. D- Appl. Phys, Vol.28, 1995, pp.2051-2059.
[13]S. Lu, H. Fujii , K. Nogi," Influence of welding parameters and shielding gas composition on GTA weld shape", ISIJ International, Vol. 45, No. 1, 2005, pp.66-70.
[14]S. Lu, H. Fujii , K. Nogi, M. Tanaka. Manabu , K. Nogi," Effects of Oxygen Additions to Argon Shielding Gas on GTA Weld Shape," ISIJ International, Vol. 43, No. 10, 2003, pp. 1590–1595.
[15] U. Reisgen, M. Schleser, O. Mokrov, E. Ahmed, "Shielding gas influences on laser weldability of tailored blanks of advanced automotive steels". Applied Surface Science, Vol. 257, 2010, pp.1401–1406.
[16] J. Sabaghzadeh, M. Azizi, M.J Torkamany, "Numerical and experimental investigation of seam welding with a pulsed laser", Optics & Laser Technology, Vol. 40, 2008, pp.289–296.
[17] Standard Test Methods for Determining Average Grain Size. E 112. vol 03.01.Philadelphia: Annual Book of ASTM Standards; 1983.
[18]National institute of standard and technology, http://physics.nist.gov/cigibin/atdata/lines_form.
[19] S. Lu, H. Fujii , K. Nogi," Marangoni convection and weld shape variations in Ar–O2and Ar–CO2 shielded GTA welding", Materials Science and Engineering A, Vol.380, 2004, pp.290-297.
[20] X. He," heat transfer, fluid flow and mass transfer in laser welding of stainless steelwith small length scale" Ph.D Thesis, The Pennsylvania State University, 2006, pp. 27-29.
[21]Y. Austin Chang and W. Alan Oates, "Materials Thermodynamics"John Wiley & Sons, New Jersey, 2010.
[22] Kou, Sindo, "Welding Metallurgy", Second ed, Wiley/ Interscience, New York, 2002 ,pp.393-410.
[23] O. M. Arselsen, Q. Grong, N. Ryum and N. Christensen, "HAZ grain growth mechanisms in welding of low carbon microalloyed steels", acta metall. Vol. 34, No. 9, 1987, pp. 1807-1815.
[24] D. A. Porter, K. E. Easterling, "Phase transformation in metals and alloys", Second Edition, Chapman & Hall, 1992, pp.293-320.